Fiber-launched ultratight photorefractive solitons integrating fast soliton-based beam manipulation circuitry

Eugenio DelRe
Dipartimento di Fisica, Universita' dell'Aquila, 67010 L'Aquila, Italy and Istituto Nazionale Fisica della Materia, Unita' di Roma "La Sapienza," 00185 Rome, Italy

Elia Palange[a)]
Dipartimento di Ingegneria Elettrica, Universita' dell'Aquila, 67040 Monteluco di Roio (L'Aquila), Italy and Istituto Nazionale Fisica della Materia, Unita' dell'Aquila, 67010 L'Aquila, Italy

Aharon J. Agranat
Department of Applied Physics, Hebrew University of Jerusalem, Jerusalem 91904, Israel

Self-integration of single-mode fiber to spatial solitons is achieved through the trapping of fiber-launched beams into ultratight high-aperture nonlinear waves in photorefractive paraelectric potassium-lithium-tantalate-niobate. This allows the integration of soliton-based circuitry and electroholography at longer nonabsorbed wavelengths, demonstrating electro-optic beam manipulation and two-mode routing capabilities. © *2004 American Institute of Physics.* [DOI: 10.1063/1.1651332]

In one of the more pioneering visions, two-dimensional spatial solitons (or optical needles) in photorefractive crystals[1] are considered the basis for optoelectronic beam handling devices, in which light confinement permeates a bulk three-dimensional electro-optic sample. This achievement holds the key to: (i) the viable integration of a host of useful bulk nonlinear/electro-optic crystals for which no present conventional waveguiding technology exists; and (ii) the projection of circuitry from the present two-dimensional to a fully three-dimensional integrated environment, of which solitonic arrays are a first result,[2] embodying one of the fundamental assets of optical technology.

Where the formation of spatial solitons is itself an indication of a self-integrated process in bulk, their subsequent integration into a fiber circuit represents an essential step toward device implementation. It implies the: (i) achievement of an intrinsically high mode matching between the fiber guided mode and the nonlinear soliton wave; and (ii) circumvention of any kind of hybrid device, such as a microlens, along the fiber-to-bulk-to-fiber cascade. This seamless transfer of the fiber circuit into, and transparently through, the crystal without spurious mode scattering implies that the waves be buttcoupled, and the crystal reproduces the confining index structure of the launching fiber. Physically, in turn, this means that the light-matter interaction mediating the optical nonlinearity must support ultratight optical needles, which involves both the nontrivial emergence of a relatively large optically driven refractive index modulation, of the order of $\Delta n \sim 10^{-3}$, and the activation of micron-level spatial scales, which can lead to secondary distortions, such as soliton-self-bending. Two possible solutions are the use of: (i) highly responsive ferroelectrics, such as strontium–barium–niobate 75; or (ii) paraelectrics near their phase-transition Curie temperature T_C. This second solution,

which we presently discuss, makes use of the strongly enhanced nonlinearity in near-transition paraelectric photorefractives, where the dielectric anomaly leads to huge values of the low-frequency dielectric constant ϵ_r. This makes even relatively weak optical coupling induce large changes in the sample refractive index through the quadratic electro-optic response $\Delta n = -(1/2)n^2 g_{\text{eff}} \epsilon_0^2 (\epsilon_r - 1)^2 E_{\text{sc}}^2$, g_{eff} being the quadratic electro-optic coefficient, and E_{sc} the soliton-supporting light-generated space-charge field.[3] More importantly, the paraelectric phase allows fast electro-optic beam manipulation via the possibility of changing the index pattern by acting through an external control field E_{ext}, which beats with slowly formed E_{sc} through the nonlinear relationship $\Delta n \propto (E_{\text{ext}} + E_{\text{sc}})^2$.[4,5] In analogy to electrically switched holograms,[4] it is sometimes referred to as soliton electroholography. In a recent effort, random beam filamentation, which can lead to low aperture solitons on large transverse scales (>10 μm), i.e., the optical wave exits into the bulk, expands to more than six times the single-mode size, and sometimes self-traps, have been reported.[6]

In this letter, we demonstrate an intrinsically matched deterministic single-mode fiber-soliton integration in biased near-transition KLTN (potassium-lithium-tantalate-niobate).[7] Our achievement is mediated by the emergence of butt-coupled ultratight [3–4 μm intensity at full width half maximum (FWHM)] needles that appear only in the very proximity of the crystal dielectric anomaly, at temperatures slightly above the ferroelectric phase-transition temperature T_C, in a condition in which charge diffusion and spontaneous polarization play a negligible role.[8] We are able to implement this achievement to demonstrate a soliton-based switch and router on a single-mode backbone, for a longer nonphotorefractive wavelength.[5]

The experimental setup is shown in Fig. 1. A continuous-wave argon-ion laser operating at $\lambda = 514$ nm is appropriately coupled into a single-mode HP 460 Nufern fiber. The

---
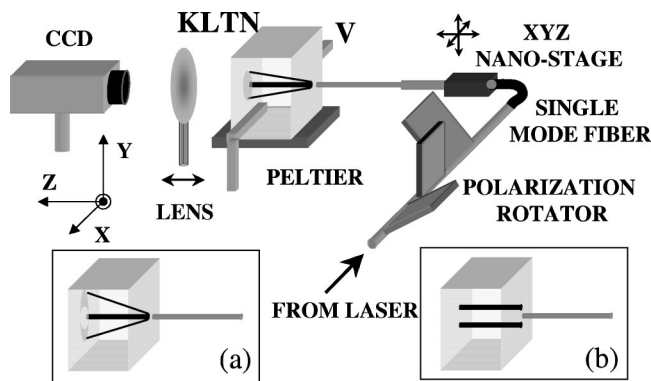[a)]Electronic mail: palange@ing.univaq.it

FIG. 1. Experimental setup: (a) Variable attenuation scheme through single soliton readout and (b) switching scheme through two vertically-stacked oppositely charged solitons.

FIG. 2. Ultratight fiber-launched needle: (a) Crystal input intensity distribution ($\Delta x = \Delta y = 3.8\ \mu$m); (b) beam diffraction at the output of the sample before soliton formation ($\Delta x = 64\ \mu$m, $\Delta y = 67\ \mu$m); and (c) Soliton output distribution ($\Delta x = 3.5\ \mu$m, $\Delta y = 4.5\ \mu$m).

fiber output is mounted on a three-axis nanopositioner providing fine alignment for its buttcoupling to the crystal input facet. The resulting polarization of the z launched beam is controlled by means of a three-stage polarization rotator. The polarization is set parallel to the applied electric field $E_{ext} = V/L$, along the x axis, where L is the distance between the two crystal electrodes. The input and output intensity distributions are collected by an $f = 20$ mm (numerical aperture $\simeq 0.5$) lens imaging the transverse $x-y$ planes onto a two-dimensional charge coupled device silicon camera DataRay WinCamD.

The crystal is a $3.7^{(x)} \times 4.1^{(y)} \times 2.4^{(z)}$ mm sample of KLTN which undergoes a ferroelectric–paraelectric phase transition at $T_C \simeq 12\,°$C.[3] Given the electro-optic geometry, $g_{eff} = g_{11} = 0.12$ m^4 C^{-2} and $n = 2.4$. The crystal manifests strong photorefraction for the $\lambda = 514$ nm beam, whereas for wavelengths longer than 600 nm, such as the He–Ne $\lambda = 633$ nm line, it becomes fully transparent. For soliton generation, the sample is kept at a constant temperature $T = 20\,°$C through a driven Peltier thermostat.

For a single-mode link, buttcoupling rigidly fixes the transverse size of the nonlinear wave. In our case, this produces an input beam $\Delta x = \Delta y = 3.8\ \mu$m, leading to the highly diffracting regime shown in Figs. 2(a) and 2(b), corresponding to 17 diffraction/nonlinear lengths. At this ul-

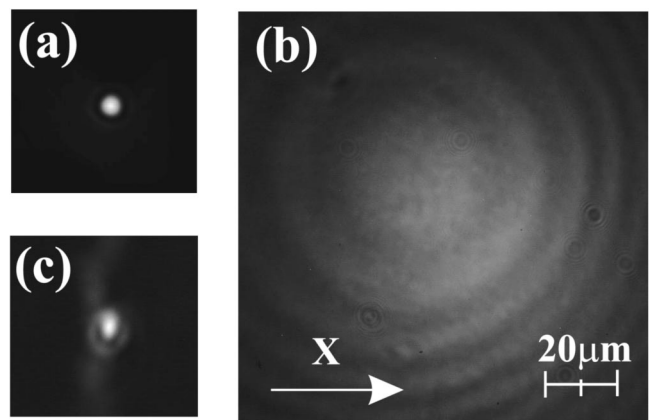tratight level, if we base our predictions on the reduced slab-soliton model,[9] which is known to, at most, underestimate needle soliton formation parameters, we obtain a minimum expected soliton supporting index modulation $\Delta n_{0,th} = (1/2)n^2 g_{eff}\epsilon_0^2(\epsilon_r - 1)^2(V/L)^2 \simeq 1.2 \cdot 10^{-3}$. In our conditions of near-phase-transition operation, the sample has an $\epsilon_r \simeq 1.6 \times 10^4$, and quasisteady-state self-trapped waves appear for values of $V = V_{sol} = 1$ kV, corresponding to an external field of $E_{ext} = E_{sol} \simeq 2.7$ kV/cm, as shown in Fig. 2(c). The wave forms for a cumulated charge separation lasting $\tau_s \simeq 70$ s for the 2.5 μW launch.[10] The resulting $\Delta n_{0,exp} \simeq \Delta n_{0,th}$ confirms the approximate prediction. Switching off the bias field (i.e., setting $V = 0$) leads to the antiguiding structure shown in Fig. 3(b), an indication of efficient electroholographic response even for these tight structures [see schematic of Fig. 1(a)]. For intermediate values of $\eta = V/V_{sol}$ the relative transmission R (normalized ratio of peak mode intensity to the $\eta = 1$ value) is also plotted in Fig. 3, and shows an effective extinction ratio of over 30 dB.

We investigated electro-optic functionality at nonphotorefractive wavelengths by launching in the very same fiber an x-polarized $\lambda = 633$ nm, 250 nW He–Ne beam, achieving automatically overlap. This constitutes a linearly propagating
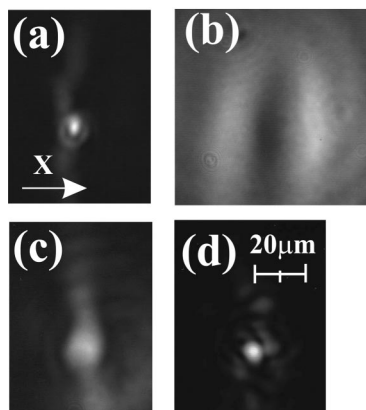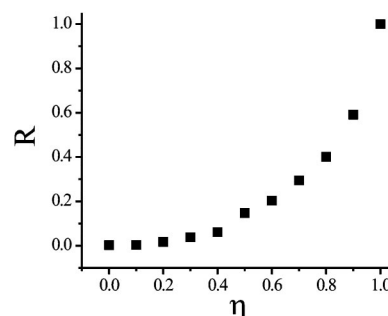

FIG. 3. Electro-optic readout: (a) The soliton output distribution at $\lambda = 514$ nm and $\eta = 1$; (b) Antiguiding output pattern $\lambda = 514$ nm and $\eta = 0$; (c) Readout at $\lambda = 633$ nm and $\eta = 1$, $T = 20\,°$C, ($\Delta x_{red} = 10\ \mu$m and $\Delta y_{red} = 18\ \mu$m); and (d) as (c) for $T = 15.5\,°$C ($\Delta x_{red} = 5.5\ \mu$m and $\Delta y_{red} = 5.3\ \mu$m). The plot shows the measured relative transmission $R(\eta)$.
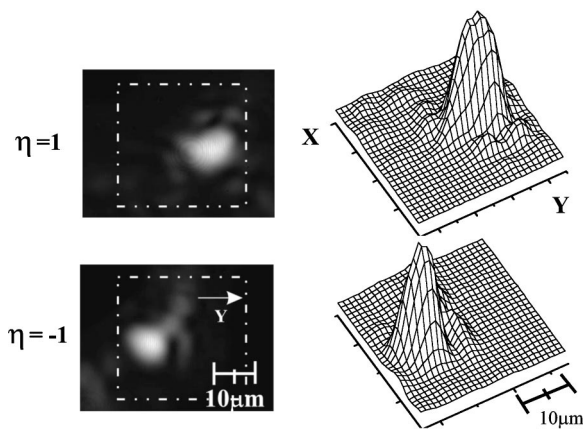
FIG. 4. Switching through opposite charged solitons. Intensity distribution (left) and mode structure (right) for the oppositely biased routing stages.

signal which does not lead to charge separation and the ensuing nonlinear manifestations. By switching on and off the soliton index pattern (i.e., by commuting η from 1 to 0), fast electro-optic switching is achieved. However, given the longer λ, guiding is less effective, as shown in Fig. 3(c), where a wide output red mode $\Delta x_{red} = 10$ μm and $\Delta y_{red} = 18$ μm is observed. Since the crystal is in near-phase transition, we have a handle on the dielectric response through the temperature dependent $\epsilon_r(T)$.[3] By lowering the crystal temperature in readout, the more confined and circular transmitted mode of Fig. 3(d) is obtained.

We went further and built a twin soliton switching device, based on two oppositely charged solitons.[5] Circuit construction was achieved by: (i) launching a soliton with $\eta = 1$ bias; (ii) raising the fiber by approximately 20 μm along y; and (iii) launching a second soliton with $\eta = -1$, as shown schematically in Fig. 1(b). Thus, a single step vertical stacking procedure was implemented.[5] During readout, the $\lambda = 633$ nm beam was launched in between the two soliton waveguides [Fig. 1(b)]. Fiber switched modes are shown in Fig. 4, and the two states correspond to $\eta = 1$ and -1, the crystal being cooled to $T = 16\,^\circ$C. The resulting switching peak-to-peak distance was 16 μm, whereas average (for the two states) mode distribution has an intensity FWHM $\Delta x_{red} = 6.5$ μm and $\Delta y_{red} = 7.8$ μm.

Tight spatial scales associated with our procedure should be accompanied by considerable bending along the propagation axis z, leading to a lateral x-directed shift.[11] In our experiments, this shift is $\simeq 6$ μm, lower than what might be expected. Apparently, the nonlinear regime activated by trapping ultratight solitons and propagating a large number of diffraction/nonlinear lengths, is different from known quasi-steady-state phenomenology.[12] For example, if we allow the process to evolve in time, after the standard soliton decay, we observe a second and third formation-decay process, each characterized by increasingly larger self-bending. The third appearance is characterized by a 22 μm output lateral shift.

As argued, fiber launching and high nonlinearity are the basis for the matched single-mode transfer from fiber-to-soliton (-to-fiber), an achievement which can impact future technological solutions in information handling. A lenient approach would be to allow for the formation, in the crystal,

of an inverted funnel linked to a substantially broader *quasisoliton*. Involving more tenable values of Δn,[6] this approach shifts the integration issue one step further, i.e., collecting the transmitted signal into the outgoing fiber, thwarting the single-mode assembly. The stringent ultratight structure, which we have demonstrated for visible beams, for standard long-haul telecommunication systems, involves a considerably higher soliton index pattern; two to three times higher than that reported here: A matter that implies operation at still higher values of ϵ_r (activating near-transition effects),[8] or adopting other soliton formation schemes. Moreover, the nonlinear nature of the link involves an initial mode adaptation that self-consistently attains the adiabatic passage from the single-mode fiber output, associated with the step-index structure, to the needle soliton wave form. How this adaptation can be (self-)induced also at the collecting end is presently under study, possibly involving counterpropagating schemes. Finally, the procedure is a demonstration that the information carrying channels can themselves be used to configure the electro-optic circuitry, by locally feeding an appropriate photorefractive signal.

In conclusion, we have demonstrated deterministic and reliable single mode fiber integration with spatial solitons through ultratight needles in photorefractives. This allows efficient electro-optic beam handling, where the fiber both carries the information sequence, and delivers the photorefractively active control beam that configures the circuitry.

[1] G. C. Duree, J. L. Shultz, G. J. Salamo, M. Segev, A. Yariv, B. Crosignani, P. DiPorto, E. J. Sharp, and R. R. Neurgaonkar, Phys. Rev. Lett. **71**, 533 (1993); M. Segev and G. Stegeman, Phys. Today **51**, 42 (1998); *Spatial Solitons* edited by S. Trillo and W. Torruellas (Springer, Berlin, 2001).

[2] J. W. Fleischer, M. Segev, N. K. Efremidis, and D. N. Christodoulides, Nature (London) **422**, 147 (2003).

[3] E. DelRe, B. Crosignani, M. Tamburrini, M. Segev, M. Mitchell, E. Refaeli, and A. J. Agranat, Opt. Lett. **23**, 421 (1998); E. DelRe, M. Tamburrini, M. Segev, E. Refaeli, and A. J. Agranat, Appl. Phys. Lett. **73**, 16 (1998).

[4] B. Pesach, G. Bartal, E. Refaeli, A. J. Agranat, J. Krupnik, and D. Sadot, Appl. Opt. **39**, 746 (2000); E. DelRe, M. Tamburrini, and A. J. Agranat, Opt. Lett. **25**, 963 (2000).

[5] E. DelRe, B. Crosignani, P. Di Porto, E. Palange, and A. J. Agranat, Opt. Lett. **27**, 2188 (2002).

[6] G. M. Tosi-Beleffi, F. Curti, D. Boschi, C. Palma, and A. J. Agranat, Opt. Lett. **28**, 1561 (2003).

[7] G. Bitton, Y. Feldman, and A. J. Agranat, Ferroelectrics **239**, 1083 (2000).

[8] E. DelRe, M. Tamburrini, M. Segev, R. Della Pergola, and A. J. Agranat, Phys. Rev. Lett. **83**, 1954 (1999).

[9] M. Segev, M. Shih, and G. C. Valley, J. Opt. Soc. Am. B **13**, 706 (1996).

[10] Use of a halted quasisteady-state process requires no extraneous stabilization procedure, such as that described in G. M. Tosi-Beleffi *et al.* Opt. Lett. **28**, 1561 (2003).

[11] M. I. Carvalho, S. R. Singh, and D. N. Christodoulides, Opt. Commun. **120**, 311 (1995).

[12] C. Denz, W. Krolikowski, J. Petter, C. Weilnau, T. Tschudi, M. R. Belic, F. Kaiser, and A. Stepken, Phys. Rev. E **60**, 6222 (1999).